المجلة العراقية للبحوث الإنسانية والإجتماعية والعلمية
Iraqi Journal of Humanitarian, Social and Scientific Research
Print ISSN 2710-0952 Electronic ISSN 2790-1254
العـــدد 17 أيـار 2025
No.17 May 2025

دور حمض التانيك كعامل اختزال وتغطية في التصنيع النباتي لجسيمات أكسيد النحاس النانوية ونشاطها المضاد للسرطان

طه علاوي أحمد
قسم علوم الحياة/ كلية العلوم/ الجامعة المستنصرية/ بغداد/ العراق.
email: taha.a.ahmed@uomustansiriyah.edu.iq
رغد ضياء عبد الجليل
قسم علوم الحياة/ كلية العلوم/ الجامعة المستنصرية/ بغداد/ العراق.
أزهار محمود حليم
مركز بحوث البيئة، جامعة التكنولوجيا، بغداد، العراق.

الملخص

في الدراسة الحالية، تم تصنيع جسيمات نانوية من أكسيد النحاس باستخدام حمض التانيك. أثناء التخليق الحيوي لجسيمات أكسيد النحاس النانوية، تحول لون الخليط من اللون الأزرق إلى اللون الرمادي. وجد طيف الأشعة فوق البنفسجية نطاقي امتصاص أقصى عند النطاقين: 215 نانومتر (λmax) و279 نانومتر لجسيمات أكسيد النحاس النانوية. كان هناك فجوتان في نطاق الطاقة: (2.8 و 3.25) إلكترون فولت والتي تشير إلى وجود آبار كمية. وجدت المجموعات الوظيفية لتحليل FTIR دليلاً على التفاعل الناجح بين حمض التانيك وجسيمات نانوية من أكسيد النحاس. كان حجم البلورة، المحسوب بمعادلة شيرير في تحليلXRD ، 20.966 نانومتر بينما كان 124.1 نانومتر عند قياسه بواسطة المجهر الإلكترونيAFM ، وكان متوسط الجذر التربيعي (Sq) 201.5 نانومتر، ومتوسط الارتفاع الحسابي 174.4 نانومتر. بالنسبة للنشاط البيولوجي، تم استخدام خط خلايا سرطان الجلد الحرشفي البشري (HSSC) وخط خلايا سرطان الفم الحرشفي البشري (HOSC) لدراسة النشاط المضاد للسرطان. في خط خلاياHOSC ، بلغ IC50 (325 و 225 و 100) ميكروجرام / مل لفترات الحضانة 24 و 48 و 72 ساعة على التوالي. بينما في خط خلايا HSSC، كانت IC50 (290 و30 و25) ميكروجرام/مل لفترات 24 و48 و72 ساعة على التوالي. في التحليل الخلوي، يعمل التركيز الأعلى من NPs على تثبيط مؤشر الانقسام mitotic index ومؤشر blast index ويسبب انحرافات كروموسومية في الخلايا الليمفاوية في الدم.

الكلمات المفتاحية: مضاد للسرطان، اوكسيد النحاس النانوي، الخلايا الليمفاوية، التصنيع النباتي، حامض التانيك.

The role of tannic acid as reducing and capping agent in phytosynthesis of copper oxide nanoparticles for anti-cancer activity

Taha A. Ahmed[1]
[1]Department of Biology/ College of Science/ Mustainsiriyah University/ Baghdad /Iraq.
email: taha.a.ahmed@uomustansiriyah.edu.iq
Raghad DHyea Abdul Jalill[2]
[2]Department of Biology/ College of Science/ Mustainsiriyah University/ Baghdad /Iraq.
Azhar M. Haleem[3].
[3]Environmental Research Center, University of Technology, Baghdad, Iraq.

Abstract

In the present study, CuO-NPs were synthesized using Tannic acid. During phytosynthesis of CuO-NPs, the color of the mixture converted from blue to grayish color. UV spectrum found two maximum absorption bands at bands: 215 nm (λmax) and 279 nm for CuO-NPs. There were two energy band gaps: (2.8 and 3.25) eV indicate to presence of quantitative wells. The functional groups of FTIR analysis found evidence for successful reaction between tannic acid and CuO-NPs. Crystal's size, calculating by Sherrer equation in XRD analysis, was 20.966 nm while it was 124.1 nm when measured by AFM, root mean square (Sq) was 201.5 nm, and arithmetic mean height 174.4 nm. For biological activity, the human skin squamous carcinoma cell line (HSSC) and human oral squamous carcinoma cell line (HOSC) were used for anticancer. In HOSC cell line, the IC50 ware (325, 225, and 100) µg/ml for the periods of incubation of 24, 48, and 72 hours, respectively. While in HSSC cell line, the IC50 were (290, 30, and 25) µg/ml for intervals of 24, 48, and 72 hours, respectively. In cytogenetic analysis, the higher concentration of NPs inhibits mitotic index, blast index and caused chromosomal aberrations in blood lymphocytes.

Keyword: Anti-cancer, CuO NPS, lymphocyte, Phytosynthesis, Tannic acid.

Introduction

In colloidal science, chemistry, physics, biology, and other scientific domains, nanotechnology is a subclassification in technology consist of study of phenomena at the nanoscale (≤ 100 nm), which differs greatly from those within a bulk material (1). The unique properties of materials at the nanoscale have the potential to bring about significant advancements in various areas of technology and industry (2). There are many kinds of nanoscale, metals nanoparticles have wide applications in biology, medicine, and engineering (3).

With a monoclinic structure and a tiny energy differential of (1–2.08) eV in the middle of the top of the valence band and the bottom of the conduction band, CuO NPs is a semiconducting compound that functions as a p-type semiconductor. Gas sensors, batteries, solar energy conversion, high-temperature superconductors, photocatalysis, heat transfer fluids, intrauterine contraceptive devices, and antifouling applications can all benefit from this characteristic (4).

CuO-NPs are highly effective against a variety of harmful microorganisms. Bacterial cells produce reactive oxygen species when exposed to high concentrations of CuO-NPs, which ultimately results in cell lysis. Additionally, CuO-NPs have demonstrated antifungal properties. (5). It used for food preservation by incorporate NPs into materials like polymers to create packaging with antimicrobial properties, improved mechanical strength, and UV-blocking capabilities (6) in addition to agricultural fields to provide defense against various harmful bacteria and fungi. Crop plants benefit from the growth and nutrients

provided by copper-based nano fertilizer and nano-insecticides. For the treatment of wastewater and the elimination of heavy metals from soil, copper-based bioremediation is essential (7).

Phytochemicals are a broad category of plant-derived chemicals, encompassing a wide variety of compounds that naturally occur in plants with diverse structures and functions (8). Unlike primary metabolites, secondary metabolites do not participate directly in growth and development. Instead, they serve various survival functions, such as plant defenses against biotic or abiotic stresses (9). Additionally, phytochemicals exhibit health-protective or disease-preventing properties (10). The main phytochemicals present in plants are flavones, terpenoids, sugars, ketones, aldehydes, carboxylic acids, and amides, some of them may be responsible for bio reduction of nanoparticles (11). Some of these Plant metabolites play important roles in the synthesis of nanoparticles and they can also be used as end-capping agents and dispersants at the same time (12). Functional groups in the extract, such as COOH, OH, NH2, CH2, CN, etc., interact electrostatically with metallic ions to reduce NPs (13)

Tannic acid is a natural polyphenol and considered as a simplest hydrolysable tannin, which occurs in a wide species of plants as a colorless to pale yellow solid with an astringent flavor, their formula: $C_{76}H_{52}O_{46}$, molecular weight is 1701.196. It serves as a food additive, conferred with exceptional properties, such as good biocompatibility, biodegradability, stimulus responsiveness, and self-healing characteristics. A short time ago, metal salts reduction by tannic acid has attracted attention of scientific community since it fulfils the requirement of a chemical redundant, but itself is a plant derived compound (14). Various natural plant are good sources of it as: the bark of oak, chestnut, hemlock, and mangrove and the leaves of certain sumacs and plant galls…. etc.(15). It has the prominent functional properties in terms of antioxidant, antimutagenic, anti-inflammatory, biodegradability, and antitumor activity (16,17)

Byun et al. created a one-step process for creating multifunctional nanoparticles using TA and causing TA and several mineral ions to self-assemble supramolecularly. Mineral-tannic acid nanoparticles (mTNs) were the result, and they were beneficial for the regeneration of bone tissue (11). Furthermore, the superior structure of TA makes it easier for them to function as a building block for supramolecularly assembled nanostructures in the field of biomedicine (19). The abundance of di-galloyl groups in particular gives TA a great chelating ability for multivalent metal ions, which causes TA to self-crosslink quickly in water to produce stable metal ion crosslinked tannic acid (MITA) nanostructures without the need for extra heat, organic solvents, chemicals, or specialized tools (20).

Remarkably, because MITA has the ability to self-regulate its adhesion, it can produce a broad range of MITA adherent materials with pH-responsive

characteristics on a number of templates (such as solid spheres, rod shapes, 2D materials, nanosheets, nanowires, nano-cubes, and hollow vesicles) that come from different sources (such as cells, proteins, bacteria, viruses, yeast, as well as polymeric and inorganic materials) (21). Current research is trying to photosynthesis of copper oxide NPs using tannic agent as capping and redacting factor, in addition to studying their toxicity to normal and cancer cells.

Materials and methods

1. **Phytosynthesis of copper oxide NPs.**

Phytosynthesis of CuO-NPs was carried out by mixing 4ml of 0.196 mM of tannic acid with the freshly prepared 2.5 ml of 1.2 mM copper sulfate solution with a continual stirring, the heating of solution was for at least 4 h at 55°C until converted of color was obtained. The fully reduced solution was further centrifuged for 15 min at room temperature (5000) rpm, washed, and stored at 4°C until further employ. The collected paste was put in a ceramic crucible cup in order to be heated in furnace at 200 °C for 2 h. and grounded to fine powder using agate mortar. The resultant white powder was put in an airtight container in order to be experimentally characterized.

For characterization, the absorption coefficient (a) and the optical band gap energy (Eg)/ UV-visible, size and distribution of NPs/ AFM, the crystal phases and crystal size / X-ray diffraction, various functional groups/ FTIR, SEM and size, grain size, size distribution and morphology/ TEM and SEM) analysis were determined.

2. Biological applications

1) Cytogenetic analysis

The culturing process was carried out to obtain chromosomes analysis according to the method mentioned in Verma and Babu 1989 (22). Healthy blood peoples cultured on (RPMI - 1640) medium. Seven different concentrations of the samples (0.0, 10, 15, 25, 50, 100, 200) µg/ml were used for analysis. The exposure time and degree temperature were: (37) °C for (2) hours. Mitotic cells MI, Blast index BI and chromosomal aberrations were calculated according to Freshney (23).

2) Hemo-compatibility test

This was done according to the Braune et al.(24) method to determined hemolysis of blood using different concentrations (0.0, 1, 5, 10, 15, 20) µg/ml of samples (24).

Cytotoxicity assay against cancer cell line

The HSSC cell line in pass 27 and HOSC cell line in pass 22 were choose for cytotoxicity assay. RPMI-1640 culture medium with all requirements supplemented was used to culture the cell line.

The MTT assay is utilized to inspect cellular metabolic activity as an indicator of cell viability, proliferation and cytotoxicity. Various concentrations of samples/ (0.0, 1, 5, 10, 15, 30, 60, 125, 250, 500, 1000) µg/mL were used for inoculation

monolayers cell lines as well described in Freshney 1992. The incubation temperature at (37°C), for different exposure periods (24, 48, 72) hours. There were triple replicates, the inhibition rate was calculated according to Freshney (23).

Statical analysis

The results were analysed statically using analysis of variance (ANOVA) with the least significant difference (LSD), and P-values at levels ($P \leq 0.01$) were deemed to be statistically significant. The SPSS version 10 program was used to perform these computations.

Results and discussion

1. Phytosynthesis

CuO-NPs were synthesized using Tannic acid. During phytosynthesis of CuO-NPs, the color of the solution mixture of copper sulfate and Tannic acid changed from blue to grayish, Figure (1). This color change indicated the reduction of metallic copper (Cu+) ions to copper oxide (CuO) NPs. The obtained material assumed as CuO-NPs was further used for physical characterizations.

Fig. (1): Color shift during phytosynthesis of NPs by tannic acid.

- **UV–visible spectroscopy**

Figure (2-A) shows two absorption band: 215 nm (λmax) and 279 nm for CuO-NPs, which confirm the formation of CuO-NPs in the solution. The absorption band of tannic acid was 260 nm (λmax)

The bandgap energy was calculated using Eg =/λ eV and found to be 2.8 and 3.25 eV Indicate the presence of quantitative wells, which is comparable to the previously reported values of energy bandgap for CuO nanoparticles, Figure (2-B).

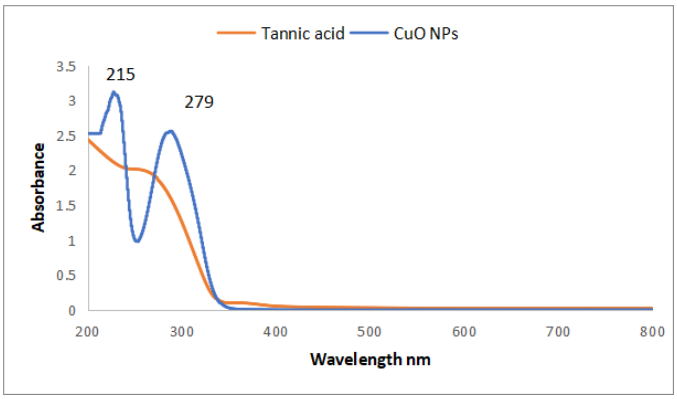

(A)

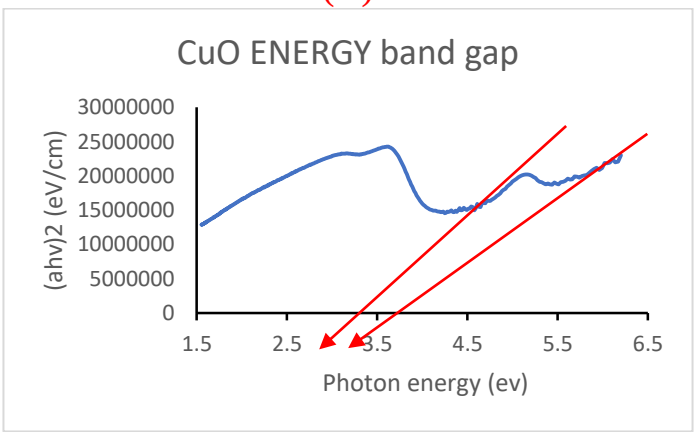

(B)

Fig. (2): (A) absorptions spectrum and (B) $(ahv)^2$ versus photon energy of NPs synthesis by tannic acid.

2. Fourier transform infrared spectroscopic analysis (FTIR)

The results of IR are determined according to NIST WEB BOOK (http://webbook.nist.gov/). The functional groups present on the surface of TA and CuO-NPs were investigated by FTIR analysis at wavelengths between 4000/cm and 400/cm Figure 3. The functional groups and their stretching which present on the surface of TA were eleven peaks: (430.12, 646, 1028/ strong C-O, 1187 /strong C-O, 1199 /strong C-O, 1400.32, 1448 C-H, 1645.28/strong C=C, 1708 /strong conjugated aldehyde C=O and 3280/ strong alkyne C-H) cm-1.

In synthesized CuO NPs, there were seven peaks (430, 621, 1028, 1111, 1354, 1620, 3412 and 3739) , their stretching are: (430/CuO , 621/CuO (25), 1028/ CuO, 1111/C–O , 1354, 1620/CuO, 3412/N-H and 3739/O-H) cm $^{-1}$ (26)

The peak observed at 3408 cm^{-1} corresponding to N–H stretching, which confirm that the polymerization occurred. It suggests that there was interaction between tannic acid and CuO nanoparticles due to presence of the same functional groups: (430 and 1620) $^{cm\ -1}$.

3. X-ray diffraction

The XRD pattern reveals the formation of a monoclinic crystalline structure by the occurrence of the well-defined diffraction peaks distinguished at 2θ = 31.912°, 35.406°, 38.673°. These distinctive peaks can be assigned to the (110), (111-), and (111-) crystallographic planes of the monoclinic structure of CuO based to the International Center for Diffraction Data (ICDD), card no. 080-1916. Other diffraction peaks were: 2h = 48.717, 58.265 and 61.526 are indexed to the (202-), (202) and (113-) crystal planes, respectively, of CuO (JCPDS card PDF file No. 48-1548), (27).

Crystal's size, strain value and dislocation density of three optimum peak are shown in (Table 1), average crystals size was: 20.966 nm.

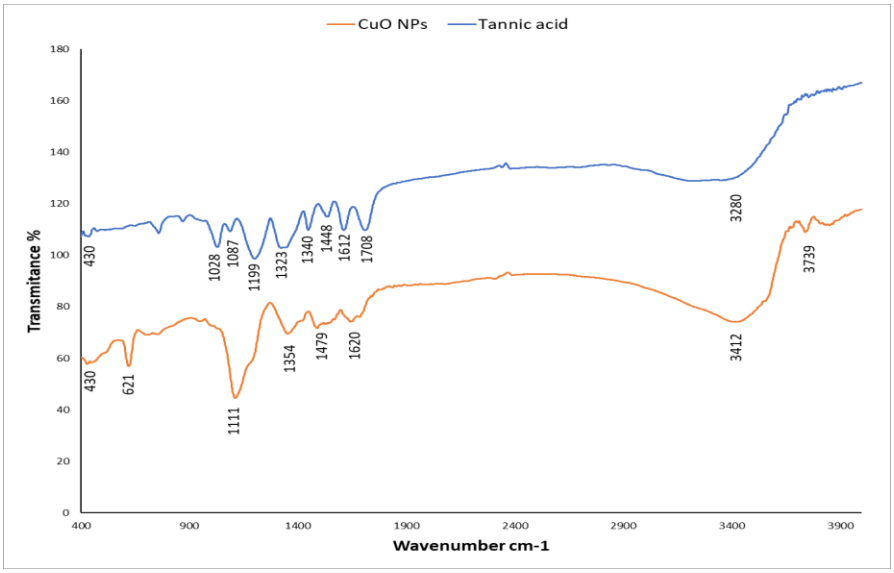

Fig. (3): FTIR analysis of NPs synthesis by tannic acid.

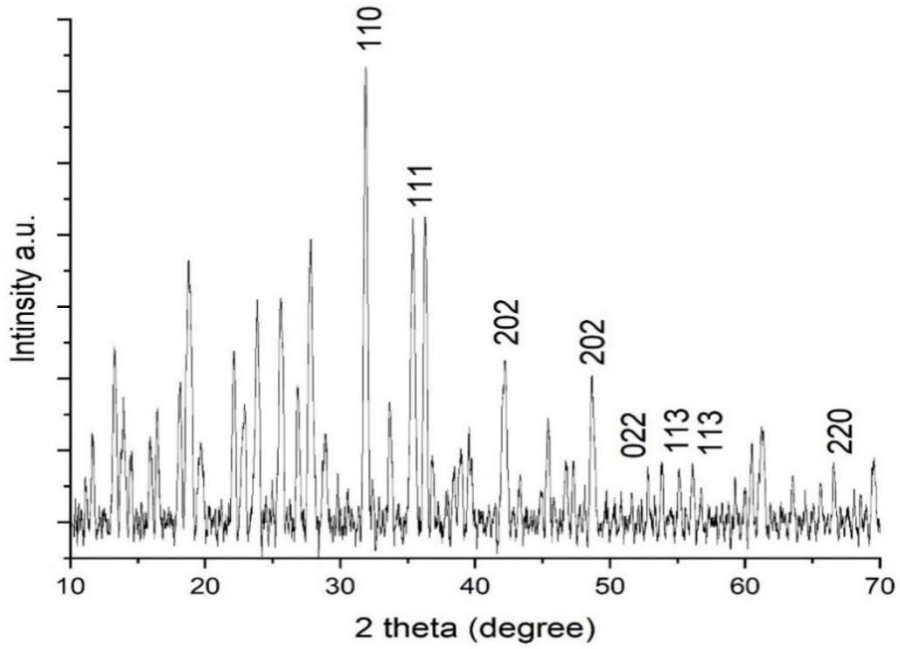

Fig. (4): X-ray pattern of NPs synthesis by tannic acid.

Table (1): XRD characterization of CuO-NPs phytosynthesis by tannic acid.

No.	Pos. [°2θ]	Plane	FWHM Left [°2θ]	D (NM)	STRAIN XE-4	DIS X1014
1	31.9116	110	0.2598	31.640	43.805	9.989
2	35.4063	002	0.433	19.162	72.330	27.234
3	38.6727	111	0.6927	12.094	114.601	68.367
Average				20.966		

(hkℓ) planes: crystallographic plane, (FWHM): Full width at half maximum, (D): dimension of crystallite size, (STRAIN $x10^{-4}$): strain value, (DIS x 10^{14}): dislocation density.

4. Zeta potential

In solution, Zeta potential test correlates to the stability of the nanoparticles, based on the surface charge of the synthesized nanoparticles (28). For example, particles with high zeta potential exhibit increased stability due to larger electrostatic repulsion between particles (29).

In this study, Zeta potential was measured at -31.03 mV as showed in Figure 5. The produced TA-CuO nanoparticles were have a moderate stability, as indicated by the larger negative zeta potential value. Phenolic compounds such as tannic acid, act as

reducing and stabilizing agents, which the researchers believe are responsible for the negative charge (30).

5. Atomic Force Microscopy

The produced CuONPs' existence and size distribution were assessed by AFM analysis. Figure (6) shows the generation of three-dimensional (3D) pictures, the average size was 124.1 nm, root mean square (Sq) was: 201.5 nm and Arithmetic mean height 174.4 nm.

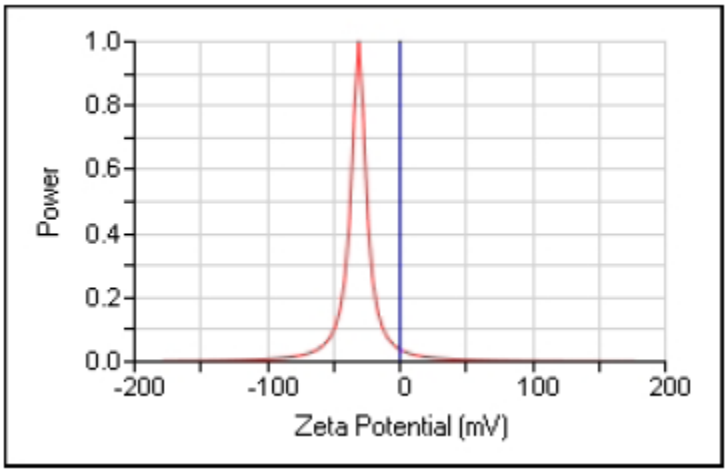

Fig. (5): Zeta potential of NPs synthesis by tannic acid.

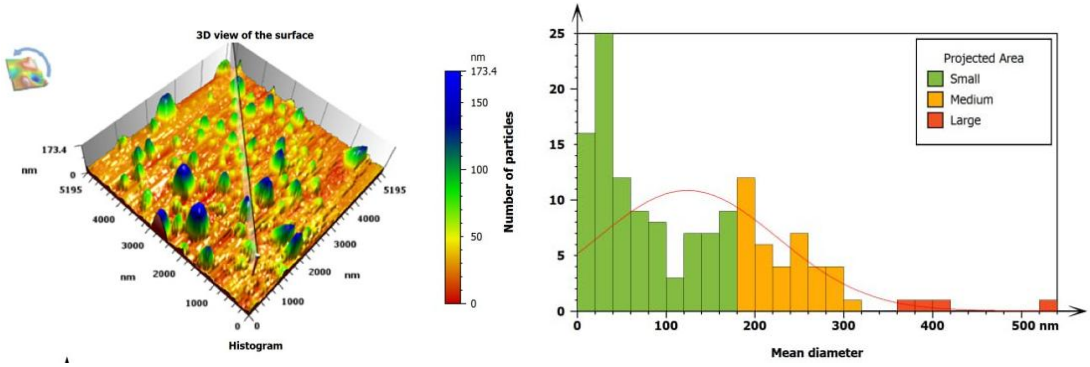

(a) (b)

Fig. (6): AFM topographic images. (a) AFM picture of CuO NPs in 3 dimensions; (b) A column AFM diagram showing volume distribution of NPs synthesis by tannic acid.

6. Scanning Electron Microscope

SEM image of CuO NPs shown in figure (7), the morphology of the CuO nanoparticles. the diameter of the CuO-NPs was determined under 66.99 nm with spherical form. In contrast to current study, the morphology of the phytosynthesized CuO-NPs was presented by Sujatha *et al.*, with similar shapes and sizes ranging between 80 and 130nm (31).

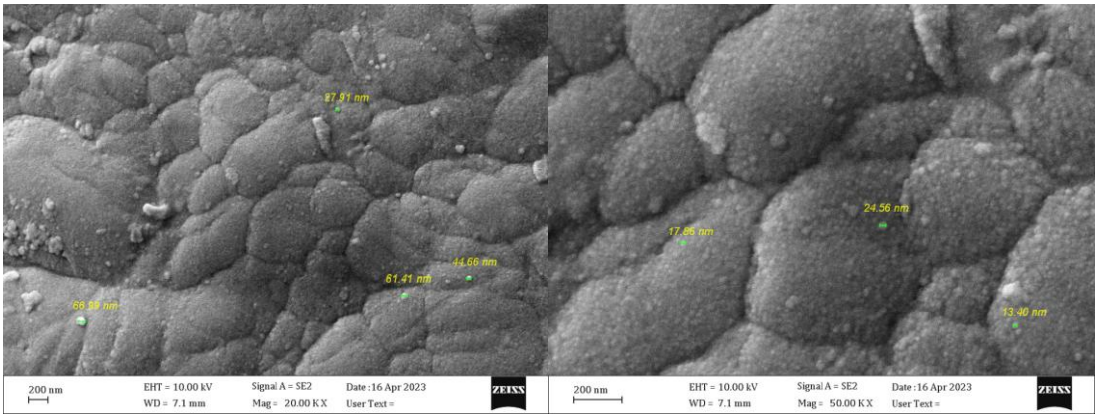

Fig. 7: SEM image of CuO-NPs synthesis by tannic acid.

7- EDX analysis

For indicating the elemental composition of CuO-NPs, the EDX analysis of the sample was carried out from the same area as shown in figure 8. The EDX analysis proves the presence of CuO-NPs produced by the phytosynthesized method. The elemental analysis of the CuO-NPs obtained 55.93% of copper and 44.07% of oxygen. According to Atri et al., the green synthesised CuO-NPs are primarily composed of Cu, O, and C with no traces of other elements, confirming that the copper oxide is pure and free of impurities (32).

2. Biological applications:

1) Cytogenetic analysis

Both the Mitotic index (MI) and blastogenic index (BI) are biological indicators approved and trusted in many studies due to their affected by endogenous and exogenous factors. Cell divisions can be considering the most important indicators of life and activity in living organisms, any physical, chemical or even biological factors that affects this physiological process can lead to the death of the organism, Therefore, these indicators can be used to determine the toxicity of substances based on the degree of their effect on these important vital indicators. The results found significant decreasing in MI and BI using all concentrations of NPs (Table 2). There were chromosomal aberrations in lymphocyte at all concentrations, significantly at the 0.01 level. MI and BI with concentrations′ raising, the significance was apparent in high concentrations more than in low concentrations. Consequently, of NPs interrelating with the structures of cell, large concentrations of metal oxides cause changes in cell cycle, resulting in phase delays which explains the decrease in both MI and BI (33).

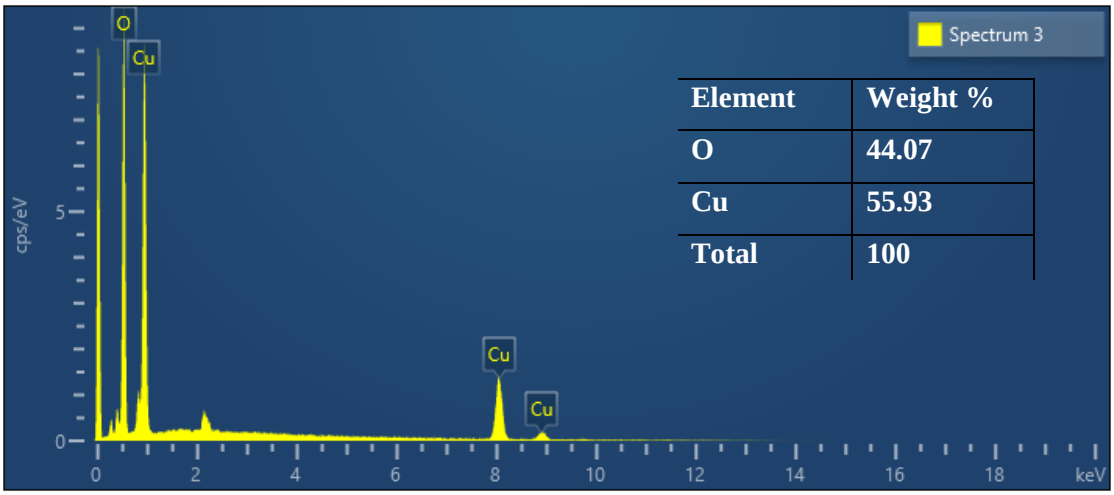

Element	Weight %
O	44.07
Cu	55.93
Total	100

Fig. 8: EDX spectrum of the CuO-NPs.

2) Hemo-compatibility test

The results of Table (3) showed cell CuO NPs interactions cause significant erythrocyte aggregation with damaging consequences, despite the NPs having significant hemolytic activity.

Nanoparticles can easily enter these cells and alter their structure and function, which may have harmful consequences. Because of this, scientists should try their best to perform comprehensive hemocompatibility studies on newly designed NPs that assess how the NPs interact with the three cellular components of blood (34). Nevertheless, it is still unclear how NPs interact with erythrocytes to induce haemolysis. Various mechanisms have been proposed, such as oxidative stress, internalization, cellular uptake, and interactions with the erythrocyte membrane. The most well-known mechanism involves NPs directly interacting with the erythrocyte membrane, which can result in cytoskeletal distortions, harmful morphological changes, and injury (35).

3) Cytotoxicity assay against cancer cell line

- **Human skin squamous carcinoma cell line.**

The results showed that all concentrations were inhibited the growth of the cancer cell line when compared with each other at (24, 48) hr., except for the high concentrations of (500, 1000) µg/ml, which the inhibitory effect did not differ significantly between themselves at (24 and 48) hr. The results also showed a sharp inhibitory effect for all concentrations used when incubated for 72 hours and compared with the control, as well as when compared with each other, except for the two concentrations 30-60 mg ml, which did not differ significantly between them, figure 9.

The IC_{50} was 290, 30, and 25 µg/ml for incubation periods of 24, 48, and 72 hours, respectively.

Table 2: Chromosomal analyses in peripheral blood lymphocytes (PBLs) treated with phytosynthetic CuO NPs.

concentration µg/ml	BI	MI	TCA
0	66.84*	1.45*	0.11*
5	61.18 *	1.19 a	0.18*
10	60.47 *	1.03 a	0.20*
15	54.48 *	0.75 b	0.25*
25	50.52 *	0.61 b	0.00 a
50	34.01*	0.39*	0.00 a
100	28.14*	0.20*	0.00 a
200	19.54*	0.00*	0.00 a

The same small letters are non-significant at the 0.01 level.

Table 3: Hemo-compatibility test.

Con. µg/mL	CuO NPs	
	Ab	H%
+ve	0.658	100
-ve	0.00	0.0
1	0.00	0.0
5	0.012	1.82
10	0.018	2.73
15	0.023	3.49
20	0.026	3.95

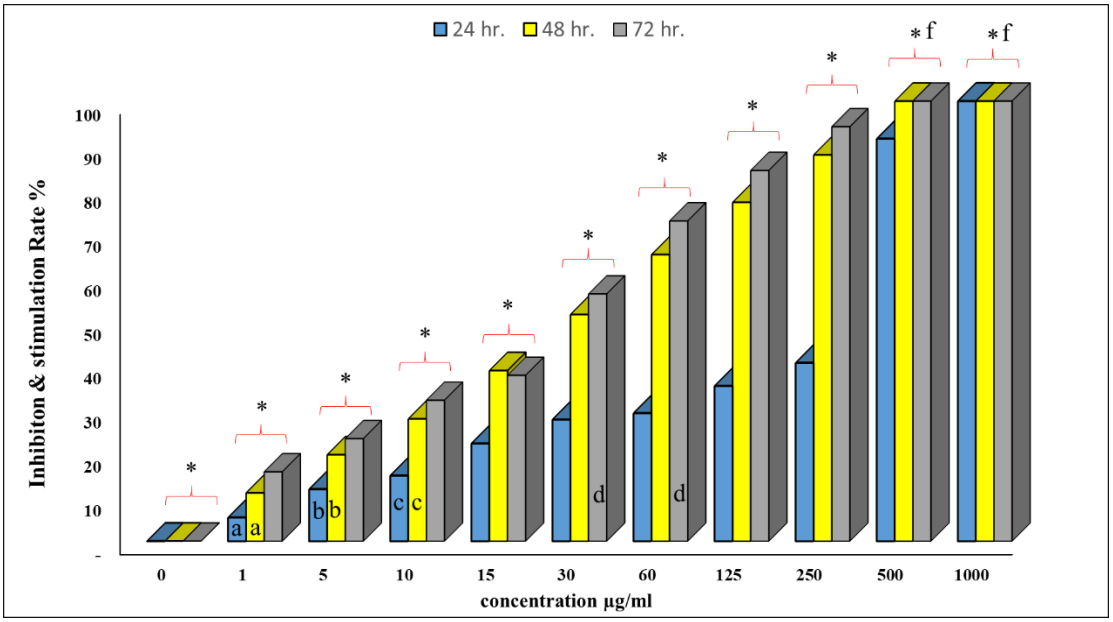

Fig. 9: Cytotoxicity assay of Phyto-synthetic CuO-NPs against human skin squamous carcinoma cell line, *: The mean difference is significant at the 0.01 level compared with all other treatments. The similar small letters are non-significant at the 0.01 level compared with the same concentration and exposure time.

- **Human oral squamous carcinoma cell line**

The control, 24 hours, is significantly different from 48 and 24 hours due to the occurrence of multiple layers. All concentrations and treatments are significantly different when compared with their controls for the periods (24, 48 and 72) hours. All concentrations between 5 µg/ml and 250 µg/ml were significantly different among themselves and also significantly different for various incubation periods. The concentrations (500 - 1000) µg/ml are significantly different from all concentrations lower than them and not significant among themselves. It remained non-significant when the incubation period progressed to 48.72 hours, meaning that the toxic effect remained the same, figure 10.

The IC_{50} was 325, 225, and 100 µg/ml for incubation periods of 24, 48, and 72 hours, respectively.

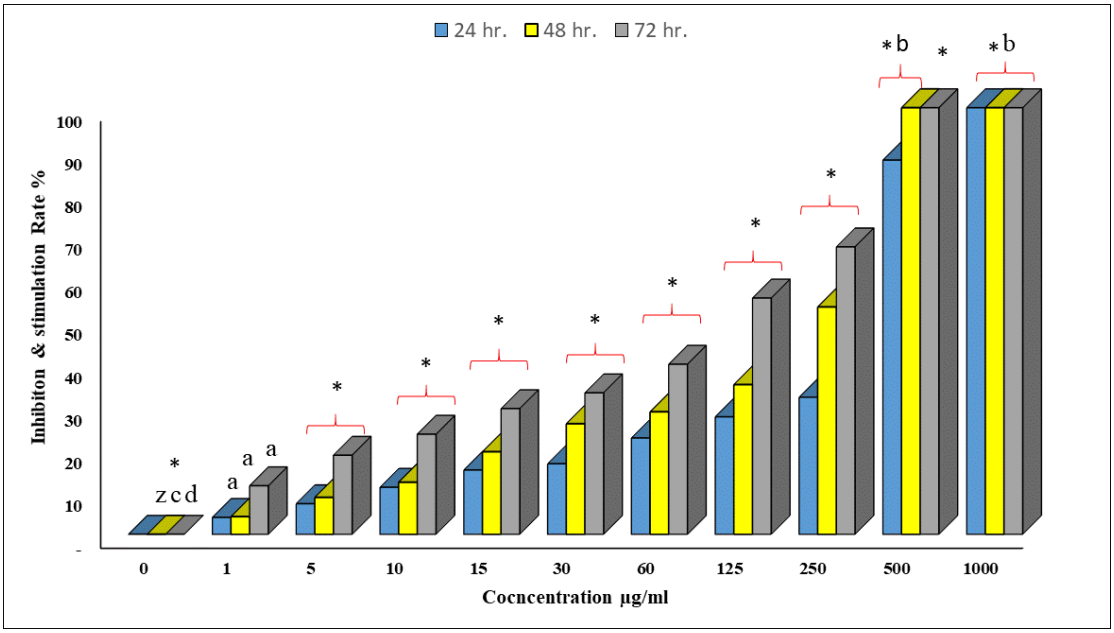

Fig. 10: Cytotoxicity assay of Phyto-synthetic CuO-Ns against human oral squamous carcinoma cell line, *: The mean difference is significant at the 0.01 level compared with all other treatments. The similar small letters are non-significant at the 0.01 level compared with the same concentration and exposure time.

Green-synthesized CuO NPs have demonstrated significant anticancer activities through various mechanisms. These nanoparticles induce apoptosis in cancer cells, as seen in studies involving pancreatic cancer cells and human lung adenocarcinoma cell lines (36,37). The apoptosis induction is often accompanied by the up-regulation of specific lncRNAs related to drug resistance, enhancing the therapeutic potential of these nanoparticles (37).

The combination of CuO NPs with other therapeutic agents can enhance their anticancer effects. For example, CuO NPs synthesized using *Aspergillus niger* extract demonstrated selective cytotoxicity towards breast cancer cells, suggesting their potential use in combination therapies for more effective cancer treatment (38).

Conclusions and Recommendations

In the present study, monoclinic structure nanoparticles of CuONPs were synthesized using Tannic acid. There is good evidence for the success of the reaction between tannic acid and CuONPs having tow energy band gaps Indicating to presence of quantitative wells.

The copper oxide nanoparticles that were prepared were inhibit the growth of HSSC cell line and HOSC at various periods of incubation of 24, 48, and 72 hours.

There were evident that the higher concentration of CuONPs found to inhibit mitotic index, blastogenic index and caused chromosomal aberrations in blood lymphocytes. Further studies can be conducted on how to reduce the toxicity of this nanomaterial by coating it with biocompatible molecules.

Acknowledgments
For its assistance with this work, the authors would like to thank Al-Mustansiriyah University (www.uomustansiriyah.edu.iq) in Baghdad, Iraq.

References:

1. Nasrollahzadeh M, Sajadi SM, Sajjadi M, Issaabadi Z. An Introduction to Nanotechnology. In 2019. p. 1–27.
2. Khan I, Saeed K, Khan I. Nanoparticles: Properties, applications and toxicities. Arabian Journal of Chemistry. 2019 Nov;12(7):908–31.
3. Santhoshkumar J, Agarwal H, Menon S, Rajeshkumar S, Venkat Kumar S. A biological synthesis of copper nanoparticles and its potential applications. In: Green Synthesis, Characterization and Applications of Nanoparticles. Elsevier; 2019. p. 199–221.
4. Boboc M, Curti F, Fleacă AM, Jianu ML, Roşu AM, Curutiu C, et al. Preparation and Antimicrobial Activity of Inorganic Nanoparticles. In: Nanostructures for Antimicrobial Therapy. Elsevier; 2017. p. 325–40.
5. Saleem MH, Ejaz U, Vithanage M, Bolan N, Siddique KHM. Synthesis, characterization, and advanced sustainable applications of copper oxide nanoparticles: a review. Clean Technol Environ Policy. 2024 Mar 13;
6. Kanithi M, Kumari L, Yalakaturi K, Munjal K, Jimitreddy S, Kandamuri M, et al. Nanoparticle Polymers Influence on Cardiac Health: Good or Bad for Cardiac Physiology? Curr Probl Cardiol. 2024 Jan;49(1):102145.
7. Gebreslassie YT, Gebremeskel FG. Green and cost-effective biofabrication of copper oxide nanoparticles: Exploring antimicrobial and anticancer applications. Biotechnology Reports. 2024 Mar;41:e00828.
8. Huang Y, Xiao D, Burton-Freeman BM, Edirisinghe I. Chemical Changes of Bioactive Phytochemicals during Thermal Processing. In: Reference Module in Food Science. Elsevier; 2016.
9. Watkins JL, Facchini PJ. Compartmentalization at the interface of primary and alkaloid metabolism. Curr Opin Plant Biol. 2022 Apr;66:102186.
10. Xiao J, Bai W. Bioactive phytochemicals. Crit Rev Food Sci Nutr. 2019 Mar 26;59(6):827–9.

11. Dwivedi AD, Gopal K. Biosynthesis of silver and gold nanoparticles using Chenopodium album leaf extract. Colloids Surf A Physicochem Eng Asp. 2010 Oct;369(1–3):27–33.
12. Ying S, Guan Z, Ofoegbu PC, Clubb P, Rico C, He F, et al. Green synthesis of nanoparticles: Current developments and limitations. Environ Technol Innov. 2022 May;26:102336.
13. Soni V, Raizada P, Singh P, Cuong HN, S R, Saini A, et al. Sustainable and green trends in using plant extracts for the synthesis of biogenic metal nanoparticles toward environmental and pharmaceutical advances: A review. Environ Res. 2021 Nov;202:111622.
14. Ahmad T. Reviewing the tannic acid mediated synthesis of metal nanoparticles. Vol. 2014, Journal of Nanotechnology. Hindawi Publishing Corporation; 2014.
15. Das AK, Islam MdN, Faruk MdO, Ashaduzzaman Md, Dungani R. Review on tannins: Extraction processes, applications and possibilities. South African Journal of Botany. 2020 Dec;135:58–70.
16. Jing W, Xiaolan C, Yu C, Feng Q, Haifeng Y. Pharmacological effects and mechanisms of tannic acid. Biomedicine & Pharmacotherapy. 2022 Oct;154:113561.
17. Baldwin A, Booth BW. Biomedical applications of tannic acid. J Biomater Appl. 2022 Mar 7;36(8):1503–23.
18. Byun H, Jang GN, Hong MH, Yeo J, Shin H, Kim WJ, et al. Biomimetic anti-inflammatory and osteogenic nanoparticles self-assembled with mineral ions and tannic acid for tissue engineering. Nano Converg. 2022 Oct 10;9(1):47.
19. Liang H, Zhou B, Wu D, Li J, Li B. Supramolecular design and applications of polyphenol-based architecture: A review. Adv Colloid Interface Sci. 2019 Oct;272:102019.
20. Huo J, Jia Q, Huang H, Zhang J, Li P, Dong X, et al. Emerging photothermal-derived multimodal synergistic therapy in combating bacterial infections. Chem Soc Rev. 2021;50(15):8762–89.
21. Liu T, Ma M, Ali A, Liu Q, Bai R, Zhang K, et al. Self-assembled copper tannic acid nanoparticles: A powerful nano-bactericide by valence shift of copper. Nano Today. 2024 Feb;54:102071.
22. Verma RS, Babu Arvind. Human chromosomes : manual of basic techniques. New York : Pergamon Press; 1989.
23. Freshney RI. Animal Cell Culture: A Practical Approach. IRL Press at Oxford University Press; 1992.

24. Braune S, Lendlein A, Jung F. Developing standards and test protocols for testing the hemocompatibility of biomaterials. In: Hemocompatibility of Biomaterials for Clinical Applications. Elsevier; 2018. p. 51–76.
25. Raul PK, Senapati S, Sahoo AK, Umlong IM, Devi RR, Thakur AJ, et al. CuO nanorods: a potential and efficient adsorbent in water purification. RSC Adv. 2014;4(76):40580–7.
26. Elango M, Deepa M, Subramanian R, Mohamed Musthafa A. Synthesis, Characterization, and Antibacterial Activity of Polyindole/Ag–Cuo Nanocomposites by Reflux Condensation Method. Polym Plast Technol Eng. 2018 Sep 22;57(14):1440–51.
27. Bin Mobarak M, Hossain MdS, Chowdhury F, Ahmed S. Synthesis and characterization of CuO nanoparticles utilizing waste fish scale and exploitation of XRD peak profile analysis for approximating the structural parameters. Arabian Journal of Chemistry. 2022 Oct;15(10):104117.
28. Jain D, Shivani, Bhojiya AA, Singh H, Daima HK, Singh M, et al. Microbial Fabrication of Zinc Oxide Nanoparticles and Evaluation of Their Antimicrobial and Photocatalytic Properties. Front Chem. 2020 Sep 30;8.
29. Keabadile OP, Aremu AO, Elugoke SE, Fayemi OE. Green and Traditional Synthesis of Copper Oxide Nanoparticles—Comparative Study. Nanomaterials. 2020 Dec 14;10(12):2502.
30. Al-darwesh MY, Ibrahim SS, Mohammed MA. A review on plant extract mediated green synthesis of zinc oxide nanoparticles and their biomedical applications. Results Chem. 2024 Jan;7:101368.
31. Sujatha J, Asokan S, Rajeshkumar S. ANTIDERMATOPHYTIC ACTIVITY OF GREEN SYNTHESISED ZINC OXIDE NANOPARTICLES USING Cassia alata LEAVES. Journal of microbiology, biotechnology and food sciences. 2018 Feb 1;7(4):348–52.
32. Atri A, Echabaane M, Bouzidi A, Harabi I, Soucase BM, Ben Chaâbane R. Green synthesis of copper oxide nanoparticles using Ephedra Alata plant extract and a study of their antifungal, antibacterial activity and photocatalytic performance under sunlight. Heliyon. 2023 Feb;9(2):e13484.
33. Abdullah S, Salman SA, Kadhim AA, Haleem A. Size Control of Ag Nanoparticles Synthesized by PLA Method in Different Liquid Environments and their Potent against Virulent Candida Albicans. J Pharm Negat Results. 2022 Jan 1;13(4).
34. de la Harpe K, Kondiah P, Choonara Y, Marimuthu T, du Toit L, Pillay V. The Hemocompatibility of Nanoparticles: A Review of Cell–Nanoparticle Interactions and Hemostasis. Cells. 2019 Oct 7;8(10):1209.

35. Chen LQ, Fang L, Ling J, Ding CZ, Kang B, Huang CZ. Nanotoxicity of Silver Nanoparticles to Red Blood Cells: Size Dependent Adsorption, Uptake, and Hemolytic Activity. Chem Res Toxicol. 2015 Mar 16;28(3):501–9.
36. Manikandan DB, Arumugam M, Veeran S, Sridhar A, Krishnasamy Sekar R, Perumalsamy B, et al. Biofabrication of ecofriendly copper oxide nanoparticles using Ocimum americanum aqueous leaf extract: analysis of in vitro antibacterial, anticancer, and photocatalytic activities. Environmental Science and Pollution Research. 2021 Jul 6;28(26):33927–41.
37. Hosseini Z, Ahmadi A, Shadi A, Hosseini SJ, Nikmanesh H. Green-synthesized copper oxide nanoparticles induce apoptosis and up-regulate *HOTAIR* and *HOTTIP* in pancreatic cancer cells. Nanomedicine. 2024 Aug 20;19(18–20):1629–41.
38. Muthukumarasamy R, Nisa ML Bin, Rosli NAB, Kamaruddin NSB, Danish M, Mahmad AB, et al. Elucidation of antibacterial, synergistic, antioxidant, and anticancer activities of green synthesized copper oxide nanoparticles against human breast cancer cells. Karbala International Journal of Modern Science. 2023 Aug 6;9(3).